

Time course of inner ear degeneration and deafness in mice lacking the Kir4.1 potassium channel subunit

Nora Rozengurt ^{a,1}, Ivan Lopez ^{b,1}, Chi-Sung Chiu ^c, Paulo Kofuji ^d, Henry A. Lester ^c, Clemens Neusch ^{c,e,*}

^a Department of Pathology, UCLA School of Medicine, Los Angeles, CA 90095, USA

^b Surgery Department, Division of Head and Neck, UCLA School of Medicine, Los Angeles, CA 90095, USA

^c Division of Biology, California Institute of Technology, Pasadena, CA 91125, USA

^d Department of Neuroscience, University of Minnesota, Minneapolis, MN 55455, USA

^e Department of Neurology, Georg-August-University, Robert-Koch Strasse 40, 37075 Göttingen, Germany

Received 6 September 2001; accepted 20 December 2002

Abstract

The Kir4.1 gene (KCNJ10) encodes an inwardly rectifying K⁺ channel subunit abundantly expressed in the CNS. Its expression in the mammalian inner ear has been suggested but its function *in vivo* in the inner ear is unknown. Because diverse human hereditary deafness syndromes are associated with mutations in K⁺ channels, we examined auditory function and inner ear structure in mice with a genetically inactivated Kir4.1 K⁺ channel subunit. Startle response experiments suggest that Kir4.1^{-/-} mice are profoundly deaf, whereas Kir4.1^{+/-} mice react like wild-type mice to acoustic stimuli. In Kir4.1^{-/-} mice, the Reissner membrane is collapsed, the tectorial membrane is swollen, and type I hair cells and spiral ganglion neurons as well as their central processes degenerate over the first postnatal weeks. In the vestibular ganglia, neuronal cell death with apoptotic features is also observed. Immunostaining reveals that Kir4.1 is strongly expressed in stria vascularis of wild-type but not Kir4.1^{-/-} mice. Within the spiral ganglion, Kir4.1 labeling was detected on satellite cells surrounding spiral ganglion neurons and axons. We conclude that Kir4.1 is crucial for normal development of the cochlea and hearing, via two distinct aspects of extracellular K⁺ homeostasis: (1) in stria vascularis, Kir4.1 helps to generate the cochlear endolymph; and (2) in spiral and vestibular ganglia, Kir4.1 in surrounding glial cells helps to support the spiral and vestibular ganglion neurons and their projecting axons.

© 2003 Elsevier Science B.V. All rights reserved.

Key words: Deafness; Inner ear; Stria vascularis; Inwardly rectifying K⁺ channel; Development; KCNJ10

1. Introduction

Inwardly rectifying K⁺ channels regulate the resting membrane potential by (a) contributing much of the resting K⁺ conductance in many cells and (b) maintaining low extracellular K⁺ via spatial buffering mechanisms (Hille, 1992; Lagrutta et al., 1996; Isomoto et

al., 1997; Reimann and Ashcroft, 1999). The Kir4.1 K⁺ channel subunit underlies the major K⁺ conductance in oligodendrocytes in the spinal cord and Müller cells in the retina (Ishii et al., 1997; Kusaka et al., 1999; Kofuji et al., 2000; Neusch et al., 2001). Kir4.1 is also the only inward rectifier known to be expressed in the stria vascularis of the inner ear to date (Hibino et al., 1997; Ando and Takeuchi, 1999). Immunohistochemical studies suggest that Kir4.1 is localized to regions of the stria vascularis near capillaries. An early report presented evidence for specific Kir4.1 expression on marginal cells (Hibino et al., 1997), although later reports show Kir4.1 expression in intermediate cells (Ando and Takeuchi, 1999; Takeuchi et al., 2001). Non-specific blockers of inwardly rectifying K⁺ channels decreased

* Corresponding author. Tel.: +49 (551) 396621;

Fax +49 (551) 398405.

E-mail address: cneusch@gwdg.de (C. Neusch).

¹ These authors contributed equally to this study.

Abbreviations: EP, endocochlear potential; ITI, inter-trial interval; PPI, pre-pulse inhibition

the endocochlear potential (EP) in vivo (Hibino et al., 1997); furthermore, Kir4.1 expression follows the time course of the developmental pattern of EP generation. These observations have led to the specific hypothesis that Kir4.1 expressed on the intermediate cells helps to generate the EP by spatially buffering K⁺ at a low level in a distinct intrastrial compartment that is transcellular from the much higher-K⁺ cochlear endolymph (Takeuchi et al., 2000, 2001). Thus Kir4.1 would help to buffer K⁺ in a low-K⁺ extracellular compartment, similar to its function in the Müller cells of the retina and probably elsewhere on glia.

This postulated role implies that animals without Kir4.1 would be deaf. To investigate further the role of the Kir4.1 K⁺ channel subunit in the ear and in other areas of the CNS, a mouse strain was developed that has a highly specific loss of the Kir4.1 gene product. Impact of this deletion on other areas of the CNS has been published elsewhere (Kofuji et al., 2000; Neusch et al., 2001). Here we report consequences of the gene inactivation for the inner ear at a behavioral and anatomical level. The hypothesis of deafness has been confirmed; furthermore, the Kir4.1 knockout mouse has pronounced anatomical anomalies in the inner ear, showing that Kir4.1 is directly or indirectly required for proper development as well as for acute auditory function. In another recent report, Kir4.1 knockout mice lack EP and have reduced K⁺ concentration in cochlear endolymph (Marcus et al., 2002).

2. Materials and methods

Experimentation on animals has been approved by the California Institute of Technology's Animal Care and Use Committee.

2.1. Targeting of the Kir4.1 subunit and polymerase chain reaction analysis

A standard gene targeting approach was chosen to disrupt Kir4.1 gene expression as described (Kofuji et al., 2000; Neusch et al., 2001). Primers for genotyping were: Kir4.1 forward 5'-GAT CTA TGG ACG ACC TTC ATT GAC ATG CAA TGG-3' and reverse 5'-GGC TGC TCT CAT CTA CCA CAT GGT AGA AAG TCA GG-3' and neomycin resistance gene forward 5'-ATC GCC TTC TAT CGC CTT CTT GAC GAG TTC TTC-3'.

2.2. Auditory startle response

Testing was conducted on wild-type (WT), Kir4.1+/- and Kir4.1-/- mice bred on a mixed genetic background. The Startle Response System (SR-LAB, San

Diego Instruments, San Diego, CA, USA) consisted of a Plexiglas cylinder (5 cm in diameter) mounted on a Plexiglas platform, in a ventilated, sound-attenuated cubicle with a high-frequency loudspeaker (28 cm above the cylinder) producing all acoustic stimuli. The background noise of each chamber was 68 dB. Movements within the cylinder were detected and transduced by a piezoelectric accelerometer attached to the Plexiglas base and digitized and stored by a computer. Beginning at the stimulus onset, 65×1 ms readings were recorded to obtain the animal's startle amplitude.

Each session was initiated with a 2 min acclimation period followed by five successive 110 dB trials of broadband noise. These trials were not included in the analysis. Six different trial types were then presented: startle pulse alone (120 dB/40 ms long), four different trials in which 20-ms-long 85, 93, 105 or 120 dB stimuli were presented and then one trial in which only the background noise was presented to measure the baseline movement in the cylinders. All trials were presented in a pseudorandom order, and the average inter-trial interval (ITI) was 15 s (10–20 s). The startle data were analyzed by two-way analysis of variance and the various stimulation intensities as the repeated measure, followed by post hoc Fisher's least significance difference test.

2.3. Histology

Animals ($n=3$) at postnatal day 6, 9 and 18 were anesthetized with halothane and cardioperfused with phosphate-buffered saline (PBS) followed by 4% paraformaldehyde (PFA) in PBS. The temporal bones were removed from the skull. The ears were immersed in a solution containing 1% glutaraldehyde/4% PFA for 1 day. Thereafter they were placed in a decalcifying solution (3% EDTA in buffered phosphate solution for 15 days) and then in 1% osmium tetroxide for 1 h.

The auditory bullae containing the cochlea and vestibular endorgans was further microdissected, dehydrated and embedded in EPON-810. The tissue was placed under vacuum for 3 h at 37°C to allow resin infiltration and thereafter polymerized at 65°C for 48 h. The cochlea was properly oriented to obtain cross-sections of the organ of Corti (mid-modiolar sections).

2 μm thick sections were obtained with a diamond knife for thick sections (Polysciences) using a Sorvall MT2 ultramicrotome. Sections were counterstained with 1% toluidine blue buffered solution, coverslipped sections were viewed and imaged in a Nikon Eclipse E800 microscope.

2.4. Immunohistochemistry and immunofluorescence

For immunohistochemistry, paraffin sections were

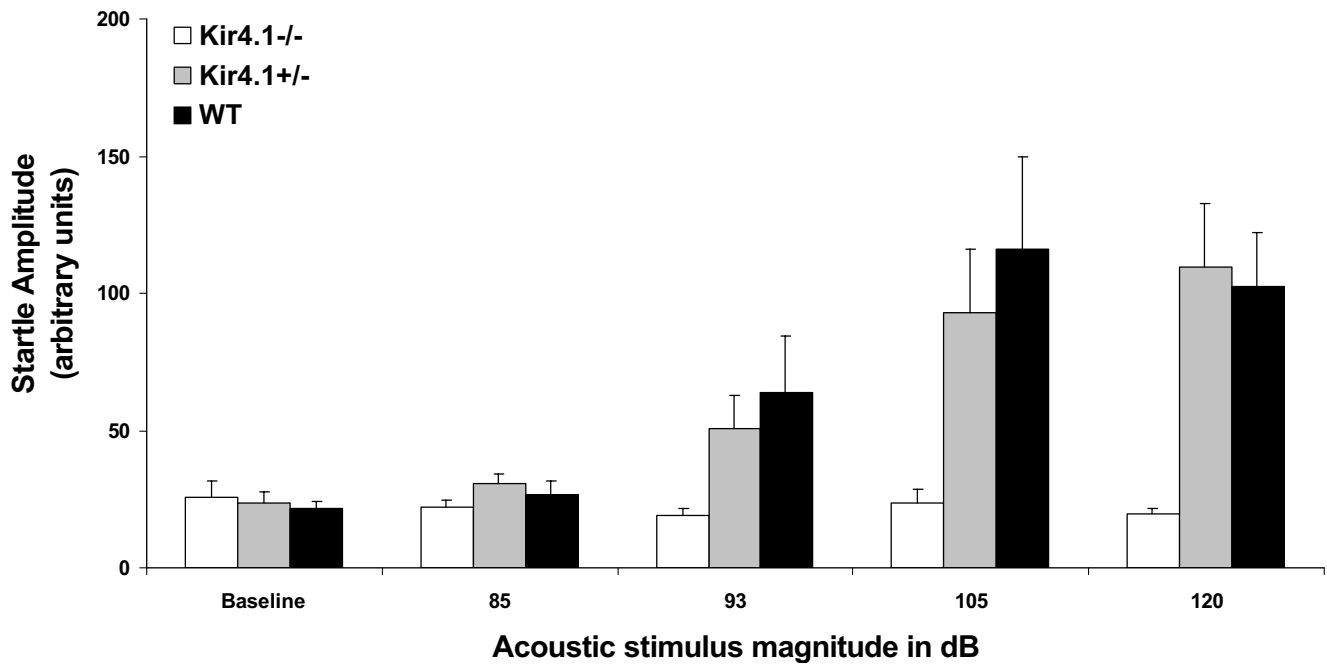


Fig. 1. Magnitude of the acoustic startle response in WT, heterozygous and Kir4.1^{-/-} mice. Mice from postnatal day 12–18 were tested. Magnitude (mean \pm S.E.M.) of the startle response (arbitrary units) to various acoustic stimuli (68 dB background noise; acoustic stimuli level ranged from 85 to 120 dB). WT mice = closed bars (number of animals, $n=9$); Kir4.1^{+/-} = striped bars ($n=6$); Kir4.1^{-/-} mice = open bars ($n=4$).

used. First, sections were dewaxed in xylene, rehydrated in ethanol and PBS, and boiled for 2 min in an antigen demasking solution (Vector Laboratories, Burlingame, CA, USA). After blocking for 15 min in 0.2% Triton X-100 and 10% normal goat serum (NGS) in PBS, samples were washed and incubated with the primary antibody in 1% NGS at 4°C overnight. Samples were incubated with a biotinylated secondary antibody followed by an avidin-conjugated fluorochrome (Vector Laboratories) or by a fluorescent (Cy-3, Alexa488)-conjugated secondary antibody alone (Jackson ImmunoResearch, West Grove, PA, USA) for 1 h. Samples were then extensively washed in PBS and analyzed first on a Nikon Epifluorescence microscope.

The anti-Kir4.1 polyclonal antibody was raised in rabbits and tested in HEK and COS cells transfected with the rat Kir4.1 subunit as described earlier (Kofuji et al., 2000). The following antibody was also used in this study: mouse-anti-cytokeratin (Chemicon, Temecula, CA, USA). Confocal images of immunostaining were obtained on a Zeiss LSM 410 microscope equipped with argon (red), HeNe (green) and UV lasers.

3. Results

3.1. Gross behavioral characterization

Kir4.1^{-/-} mice present a general underdevelop-

ment: they gain less weight than their Kir4.1^{+/-} and WT littermates. Death occurs at 9–21 postnatal days. On a behavioral level, 8–10 days postnatally, mice homozygous for the mutation develop a severe motor impairment with difficulties righting themselves. This behavior could be attributed to a severe defect in spinal cord and brainstem myelination as well as to vacuolation of deep cerebellar nuclei at early stages of development (Neusch et al., 2001). Circling behavior, head tilting or other signs of the classical Shaker/Walzer phenotype were not observed, but upon examination Kir4.1^{-/-} mice failed to show signs of startle.

Therefore Kir4.1^{-/-}, Kir4.1^{+/-} and WT mice were tested systematically for their startle response (Fig. 1). Kir4.1^{-/-} mice exhibited a total loss of startle response, in contrast to heterozygotes and WT animals. Although control animals exhibited a significant startle response to a 93 dB stimulus, Kir4.1^{-/-} mice showed no startle response at the highest stimulus strengths tested (120 dB). The pre-pulse inhibition (PPI) assay was not performed due to non-responsive Kir4.1^{-/-} animals to acoustic stimuli. These results suggest that the Kir4.1 knockout mice have compromised inner ear function, although we cannot rule out additional defects at more central levels in the auditory startle circuitry. A generalized defect in the motor system is excluded by the fact that the Kir4.1^{-/-} animals startled appropriately to tactile stimuli, such as air puffs.

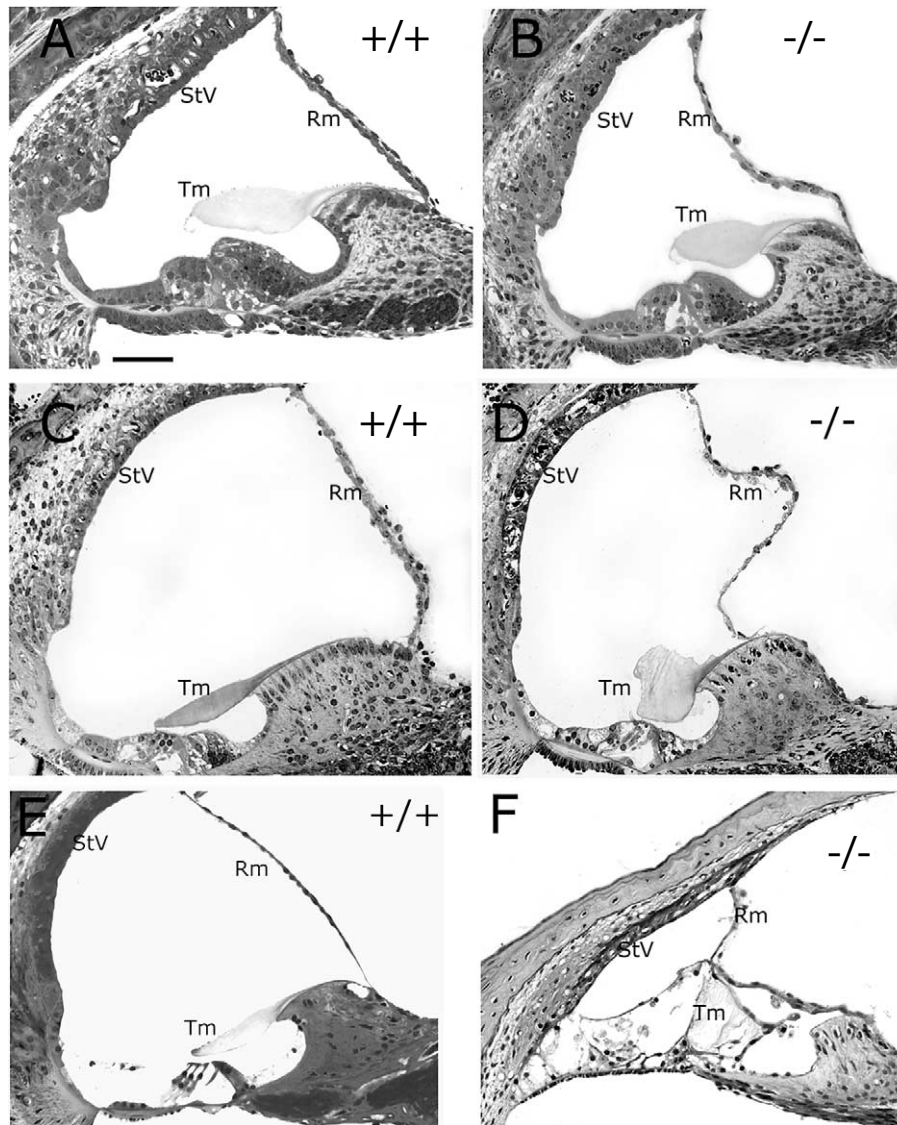


Fig. 2. Histological analysis of the cochlear duct of Kir4.1^{+/+} and ^{-/-} mice. Panels A, C and E illustrate the normal morphology of the mid-apical turn of the cochlea of Kir4.1^{+/+} mice of P6, P9 and P18 days of age. Panels B, D and F illustrate the mid-apical turn of the cochlea of Kir4.1^{-/-} mice at respective postnatal ages. At P6 (panel B), the Reissner membrane (Rm) appeared distended, while other structures appeared normal. At P9 (panel D), the stria vascularis (StV) and Reissner's membrane showed marked atrophy and the tectorial membrane (Tm) was swollen. At P18 (panel F), the organ of Corti, the tectorial membrane, Reissner's membrane and the stria vascularis were atrophic. Scale bar = 50 μ m.

3.2. Collapse of the scala media compartment and degeneration of central processes of spiral ganglion neurons and loss of spirallvestibular ganglion neurons

We examined the anatomy of the inner ear of Kir4.1^{+/+} and ^{-/-} animals at postnatal day 6, 9 and 18 (referred to as P6, P9 and P18). The WT animal control showed normally developed inner ear structures from P6 to P18 (Fig. 2A,C,E). Kir4.1^{-/-} animals clearly demonstrated pathological changes at the apical, medial and basal cochlea.

At P6 only subtle changes were observed in Kir4.1^{-/-}

— animals, while the organ of Corti was normal in appearance. Both epithelial layers of the Reissner membrane showed degenerative changes. Necrotic cells were abundant in both the endolymphatic cuboidal epithelium lining the cochlear duct and in the perilymphatic squamous epithelium. The former is discontinuous and the latter shows exfoliation of cells (Fig. 2B).

At P9, the tectorial membrane showed signs of swelling and disorganization in the direction of the fibers as compared to control animals. The Reissner membrane was progressively atrophic with sections of it reduced to the basal membrane or to a single squamous epithelium on either side of the basal membrane. Some atypically

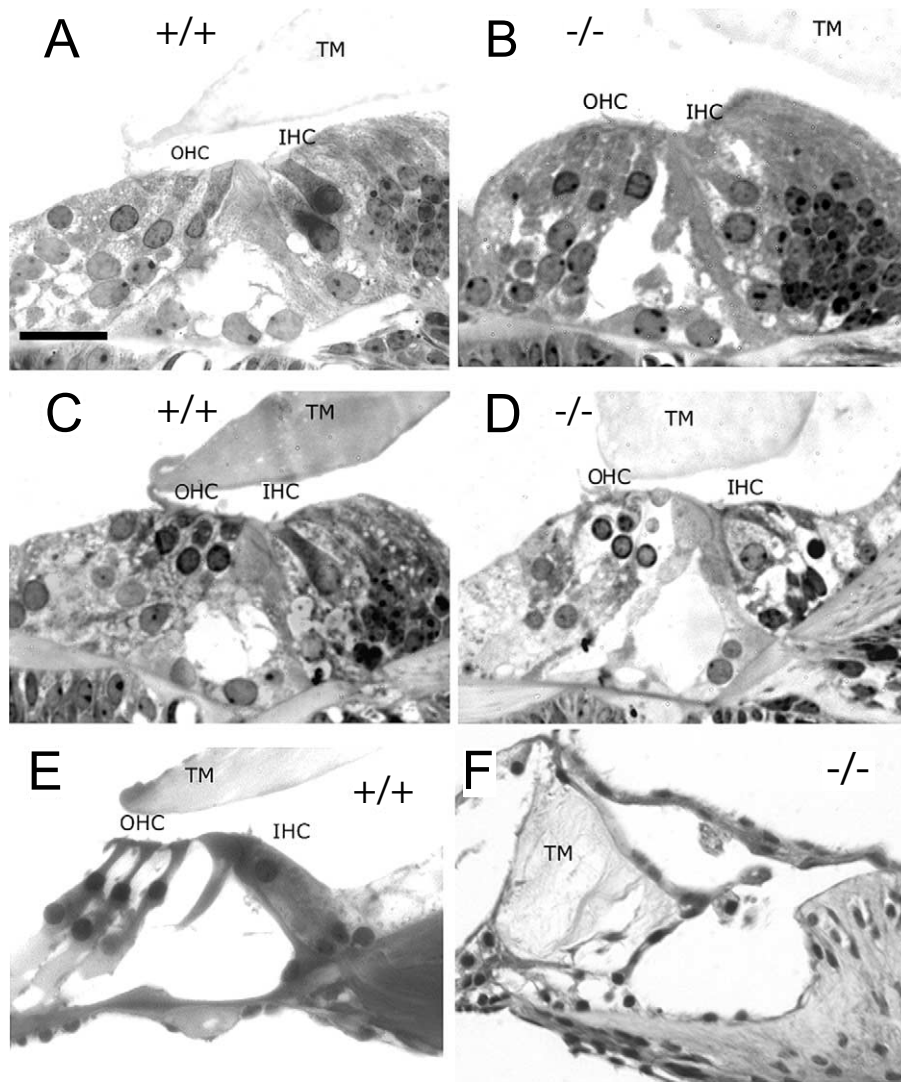


Fig. 3. Higher magnification of Fig. 2 to illustrate the organization of the organ of Corti in *Kir4.1*^{+/+} and *-/-* mice. (A,C,E) Normal morphology of the organ of Corti of *Kir4.1*^{+/+} mice of P6, P9 and P18 days of age. (B,D,F) The organ of Corti of *Kir4.1*^{-/-} mice at respective postnatal days. In *Kir4.1*^{-/-} mice at P6 (B), the outer (OHC) and inner hair cells (IHC) and surrounding supporting cells were normal in appearance, also the tectorial membrane (Tm) seemed unaffected. Panel D shows *Kir4.1*^{-/-} mice at P9; the outer and inner hair cells showed signs of atrophy (their cytoplasm was vacuolated), also the tectorial membrane appeared progressively atrophic. Panel F illustrates *Kir4.1*^{-/-} mice at P18 showing a complete absence of inner and outer hair cells and a completely atrophic tectorial membrane. Scale bars = 20 μ m.

enlarged clear nuclei were found on the cochlear side of the basal membrane and the stria vascularis also showed signs of shrinkage and atrophy. At P18, Reissner's membrane was collapsed and subsequently almost aligned onto the stria vascularis, narrowing the scala media compartment. The tectorial membrane was markedly swollen and a trichrome stain showed that the direction of the fibers was irregular, undulating and crisscrossing, in contrast to the regular parallel arrangement seen in the WT mice.

Fig. 3 compares development of the organ of Corti in WT (Fig. 3A,C,E) and *Kir4.1*^{-/-} animals. At P6, no obvious changes of the organ of Corti were observed (Fig. 3B) in *Kir4.1*^{-/-} animals; however, at P9 the

inner and outer hair cells showed signs of degeneration (Fig. 3D). By P18, the inner and outer hair cells were absent in *Kir4.1*^{-/-} sections of the cochlea (Fig. 3F). The tectorial membrane was swollen and completely disrupted (Fig. 3F).

Histological analysis of the spiral ganglia neurons of the *Kir4.1*^{-/-} animals (Fig. 4B,C) demonstrates no obvious alteration as compared with WT animals up to P9 (Fig. 4A). The cytoplasm and peripheral processes of these neurons seem to be unaffected. However, we found cell loss on the order of 50% in spiral ganglion neurons at P18 (Fig. 4F).

The central processes in the internal auditory canal (processes that are surrounded by glial cells) showed

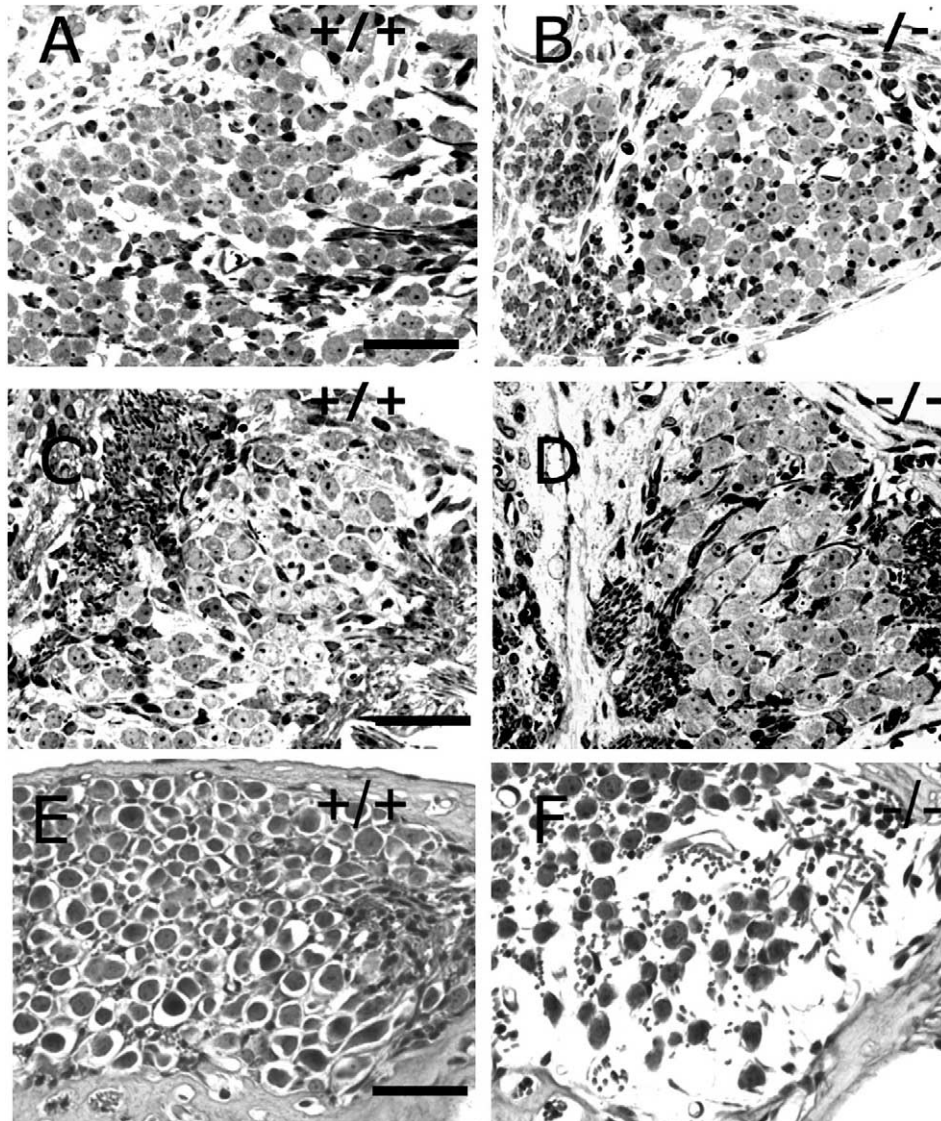


Fig. 4. Spiral ganglia neurons and fibers in the *Kir4.1*^{+/+} versus *Kir4.1*^{-/-} mice. (A,C,E) *Kir4.1*^{+/+} mice. (B,D,F) *Kir4.1*^{-/-} mice at P6, P9 and P18, respectively. The cytoplasm of *Kir4.1*^{-/-} neurons is normal in appearance as well as their peripheral processes when compared with *Kir4.1*^{+/+} mice at P6 and P9. However, there is considerable loss of neurons and surrounding non-neuronal cells in *Kir4.1*^{-/-} mice at P18 (panel F). Magnification bar = 30 μ m.

severe atrophy, i.e. the cochlear nerve bundle is atrophic (Fig. 5A).

The vestibular ganglia showed marked degeneration, some neurons have apoptotic nuclei and in certain areas neuronal cell bodies are missing (Fig. 5B). This change is reflected in the atrophy of the vestibular sensory epithelia, where thick nerve fibers from the vestibular ganglia neurons penetrate the sensory epithelia and normally surround the type I hair cells forming a calyceal terminal (Fig. 5C). Interestingly, mainly the type I hair cells showed apoptotic nuclei, while type II hair cells that are not innervated by vestibular ganglia neurons to form calyceal terminals appeared normal. All these changes were observed in the macula utriculi/sacculi, as well as in the cristae ampullaris.

3.3. *Kir4.1* expression in the postnatal mouse inner ear

A lack of *Kir4.1* has major effects on inner ear development (above), but where is *Kir4.1* expressed in the inner ear? With immunostaining, we observed high levels of *Kir4.1* expression in the stria vascularis and the satellite cells of the spiral ganglion, as well as weak labeling on Deiters' cells surrounding the outer hair cell layer (Fig. 6A,B). *Kir4.1* expression was not apparent by immunohistochemistry on sections of *Kir4.1*^{-/-} mouse inner ear at P18, showing that the mutation successfully eliminated *Kir4.1* protein expression (Fig. 6C). Within the stria vascularis, *Kir4.1* labeling partly overlapped with cytokeratin staining, suggesting that marginal cells express *Kir4.1* (Fig. 6D–I). Furthermore,

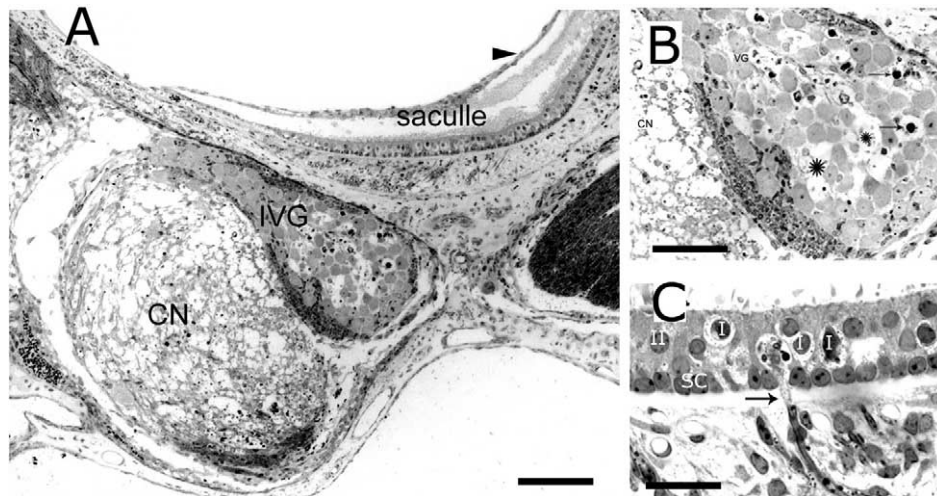


Fig. 5. Cross-section of the inner ear of a representative *Kir4.1*^{-/-} P9 animal. (A) The area of the internal auditory canal containing the cochlear nerve bundle (CN), the inferior vestibular ganglia (IVG) and macula sacculi. Arrowhead points to the saccular membrane, which is collapsed. Notice the marked atrophy in the VIIIth nerve bundle. (B) The inferior vestibular ganglion at higher magnification. Arrow points to apoptotic nuclei, asterisks show areas where vestibular neurons are missing. (C) Cross-section of the macula utriculi showing the sensory epithelium Type I (I) hair cells with pycnotic nuclei. Type II (II) hair cells and supporting cells (SC) appear normal. Arrow points to thick nerve fibers penetrating the sensory epithelium; there are signs of atrophy in this structure. Bar in panel A = 250 μ m, in panel B = 125 μ m, in panel C = 20 μ m.

most intense *Kir4.1* staining was observed in close proximity to capillaries. However, given the close association of intermediate and marginal cells in the stria vascularis, our technique lacks the sensitivity to clarify this issue.

4. Discussion

Thus far human hereditary deafness syndromes have been largely associated with mutations in outwardly rectifying, voltage-gated (K_v , K_vLQT) K^+ channels (Vetter et al., 1996; Romey et al., 1997; Schulze-Bahr et al., 1997; Wollnik et al., 1997; Wang et al., 1998; Chen et al., 1999; Talebizadeh et al., 1999; Van Hauwe et al., 1999; Chouabe et al., 2000; Kharkovets et al., 2000). Here we report that disruption of a gene encoding an inwardly rectifying K^+ channel can lead to deafness in a mammalian system. The present study provides an *in vivo* confirmation of the prediction, based on the localization of *Kir4.1* (Hibino et al., 1997; Ando and Takeuchi, 1999; Takeuchi et al., 2001), that a *Kir4.1* knockout mouse would be deaf. This deafness is accompanied by severe structural changes: the scala media compartment is collapsed, tectorial membrane is swollen and partly disrupted, and spiral/vestibular ganglion neurons degenerate.

4.1. *Kir4.1* in the stria vascularis

Our study reveals that *Kir4.1* exerts a critical role in the development of the cochlea and suggests a role in

generating the cochlear endolymph and therefore the EP. The temporal and spatial expression pattern of *Kir4.1* is appropriate for such a role: *Kir4.1* is strongly expressed in the stria vascularis. The present highly specific results are a satisfactory extension of previous studies showing that *Kir4.1* expression follows the time course of the EP generation and that non-specific pharmacological blockade of *Kir* channels, or depolarization by increased K_0 , affect EP generation and development *in vivo* (Hibino et al., 1997). These concepts are supported by the recent report that *Kir4.1* knockout mice lack EP and have reduced K^+ concentration in cochlear endolymph (Marcus et al., 2002).

Formation of the high K^+ endolymph is a multistep process, involving several pumps, transporters and channels on serially disposed membranes in the stria vascularis (Takeuchi et al., 2000). The process involves at least two K^+ channels whose genetic ablation causes collapse of the scale media, presumably because insufficient or incorrect endolymph is produced. The first of these reported channels is the heteromeric voltage-gated *ISK/KvLQT1* channel (Vetter et al., 1996; Lee et al., 2000); now, the second is an inwardly rectifying K^+ channel including the *Kir4.1* subunit. Because *Kir4.1* hetero-oligomerizes with other *Kir* subunits *in vitro* (Lagrutta et al., 1996; Xu et al., 2000; Yang et al., 2000), we believe it likely that the channels contain *Kir4.1* in association with other *Kir* subunits.

Kir channels are open at resting membrane potentials of excitable as well as non-excitable cells. Inward rectifiers in the CNS maintain K^+ homeostasis, temporally and spatially buffering K^+ . In the stria vascularis *Kir4.1*

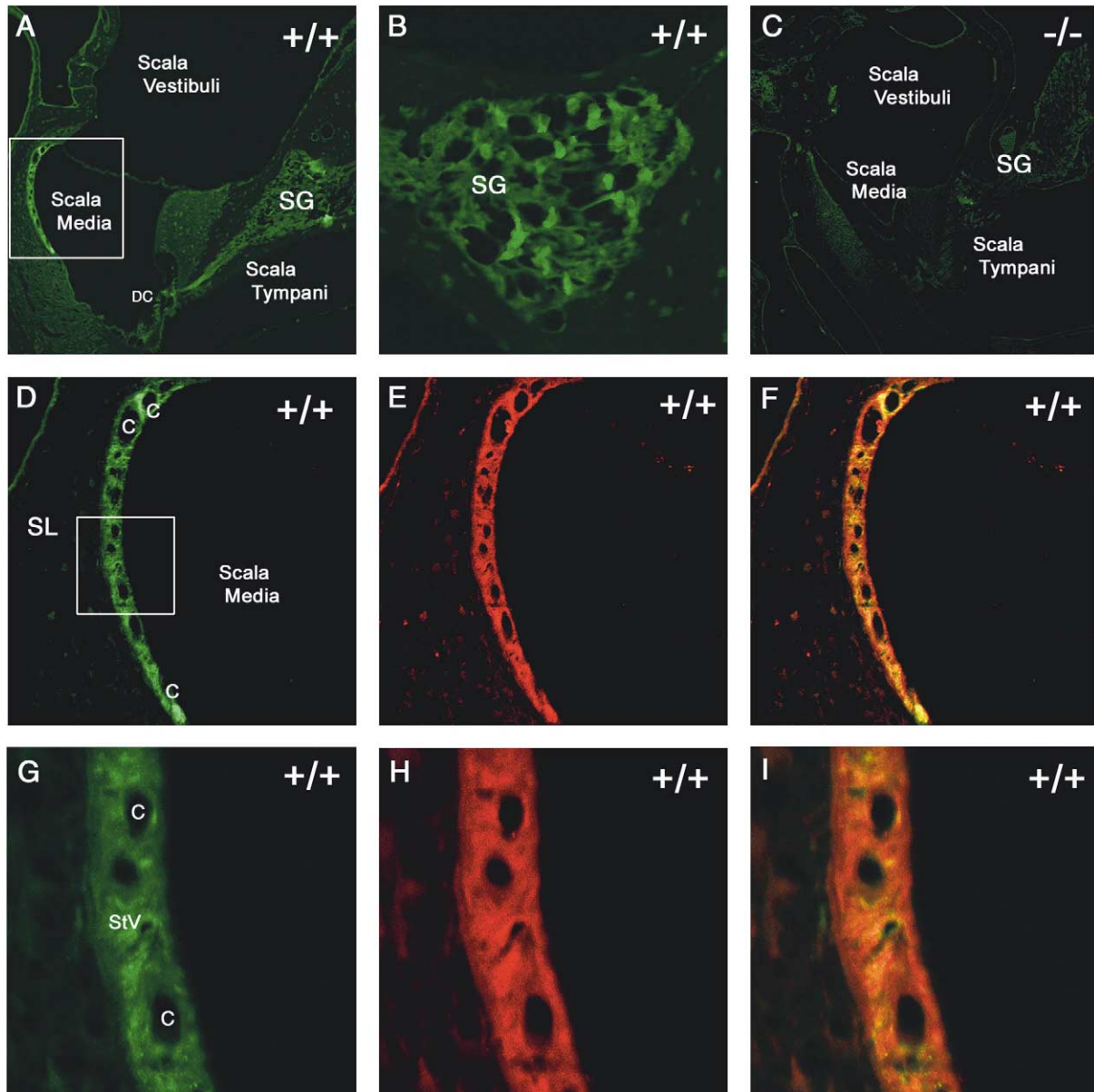


Fig. 6. Regional and cellular expression of the Kir4.1 channel subunit in sections of the cochlea as revealed by immunostaining. (A) Overview showing a transverse section of the cochlea of a WT mouse at P18. Kir4.1 labeling was observed in the stria vascularis, in the spiral ganglion, and weakly on Deiters' cells. (B) Higher power magnification of Kir4.1 immunoreactivity in the spiral ganglion of a WT mouse. (C) No immunoreactivity was observed in a Kir4.1^{-/-} mouse, showing that Kir4.1 gene expression was successfully inactivated. (D–F) Inset of panel A. In WT mice immunoreactivity for both Kir4.1 (panel D, green) and cytokeratin (panel E, red) was detected within the stria vascularis. (F) Overlay. (G–I) Inset of panel D. Note that Kir4.1 labeling (panel G) is concentrated mainly around capillaries and partly overlaps with cytokeratin immunoreactivity (panel H). (i) Overlay of confocal images. DC, Deiters' cells; SG, spiral ganglion; C, capillaries; StV, stria vascularis; SL, spiral ligament. Scale bars: panels A,C, 100 μ m; panel B, 40 μ m; panels D–F, 20 μ m; panels G–I, 10 μ m.

is expressed in close proximity to capillaries and could function in this compartment as in Müller cells of the retina, where Kir4.1 siphons K⁺ away from the neuronal environment to the vitreous humor and into vessels (Kofuji et al., 2000).

4.2. Kir4.1 in the spiral and vestibular ganglion

Central processes of spiral ganglion neurons in

Kir4.1^{-/-} mice degenerate, and there is severe degeneration in the VIIIth nerve, which contains their axons. Kir4.1 expression on spiral ganglion neurons has not been reported and was not detected in the present study. On the other hand, we did find high levels of Kir4.1 expression on the satellite cells which surround the neurons and axons of the spiral ganglion. These findings agree with earlier studies showing that Kir4.1 is specifically localized on myelin sheaths of satellite

cells wrapping the somata of ganglion neurons, and that the time course of Kir4.1 expression followed the development of action potentials of the auditory nerve (Hibino et al., 1999).

Our results show that spiral ganglion neurons and their axons as well as neurons of the vestibular ganglia degenerate, although Kir4.1 is expressed on surrounding supporting cells that myelinate the axons. These results are consistent with our previous finding that spinal cord neurons and their axons in Kir4.1^{-/-} mice degenerate, although Kir4.1 is expressed primarily on oligodendrocytes (Neusch et al., 2001). As in the previous study, we suggest that neuronal/axonal degeneration is secondary to inadequate K⁺ siphoning or other metabolic support by the poorly functioning Kir4.1^{-/-} satellite cells whose somata neighbor the neuronal cell bodies and whose processes surround their axons. The similarities between the pathology in the inner ear and in the spinal cord lead us to predict that the detailed physiology of Kir4.1 in oligodendrocytes also applies to the satellite cells: Kir4.1-containing channels would be the principal inwardly rectifying K⁺ channels in satellite cells, would set the resting membrane potential in these cells, and would be the major mechanism for siphoning away extracellular K⁺ that is released during activity. Whether the neurons or satellite cells display apoptosis has yet to be determined, though on a histopathological level, we could detect nuclei with typical apoptotic features.

Additionally, we detected weak Kir4.1 labeling on Deiters' cells surrounding the outer hair cell layer. This indicates that the channel is located near or surrounding neuronal cells of the organ of Corti. Our study reveals progressive degeneration of inner and outer hair cells. Whether this is due to disturbed function of Deiters' cells or a secondary phenomenon to the observed degeneration of innervating spiral ganglia neurons remains open.

Thus, the pathology of the Kir4.1^{-/-} mouse agrees with the spatial and temporal distribution of Kir4.1, suggesting that Kir4.1 has two major roles in the inner ear. First, it is an important membrane component of the stria vascularis, the organ regulating the generation and maintenance of the endolymph inside the scala media. Second, Kir4.1 is the major K⁺ channel in glial cells surrounding spiral ganglion neurons and axons, and possibly in epithelial cells which surround hair cells, allowing these cells to support these excitable cells.

Acknowledgements

We thank Sami Barghshoon for help with animals. This work was supported by grants from the National

Institutes of Health (GM-29836, EY12949), and the Deutsche Forschungsgemeinschaft (NE-767/1-1).

References

- Ando, M., Takeuchi, S., 1999. Immunological identification of an inward rectifier K⁺ channel (Kir4.1) in the intermediate cell (melanocyte) of the cochlear stria vascularis of gerbils and rats. *Cell Tissue Res.* 298, 179–183.
- Chen, Q., Zhang, D., Gingell, R.L., Moss, A.J., Napolitano, C., Priori, S.G., Schwartz, P.J., Kehoe, E., Robinson, J.L., Schulze-Bahr, E., Wang, Q., Towbin, J.A., 1999. Homozygous deletion in KVLQT1 associated with Jervell and Lange-Nielsen syndrome. *Circulation* 99, 1344–1347.
- Chouabe, C., Neyroud, N., Richard, P., Denjoy, I., Hainque, B., Romey, G., Drici, M.D., Guicheney, P., Barhanin, J., 2000. Novel mutations in KVLQT1 that affect I_{Ks} activation through interactions with Isk. *Cardiovasc. Res.* 45, 971–980.
- Hibino, H., Horio, Y., Inanobe, A., Doi, K., Ito, M., Yamada, M., Gotow, T., Uchiyama, Y., Kawamura, M., Kubo, T., Kurachi, Y., 1997. An ATP-dependent inwardly rectifying potassium channel, KAB-2 (Kir4.1), in cochlear stria vascularis of inner ear: its specific subcellular localization and correlation with the formation of endocochlear potential. *J. Neurosci.* 17, 4711–4721.
- Hibino, H., Horio, Y., Fujita, A., Inanobe, A., Doi, K., Gotow, T., Uchiyama, Y., Kubo, T., Kurachi, Y., 1999. Expression of an inwardly rectifying K(+) channel, Kir4.1, in satellite cells of rat cochlear ganglia. *Am. J. Physiol.* 277, C638–C644.
- Hille, B., 1992. *Ionic Channels of Excitable Membranes*, 2nd edn. Sinauer, Sunderland, MA.
- Ishii, M., Horio, Y., Tada, Y., Hibino, H., Inanobe, A., Ito, M., Yamada, M., Gotow, T., Uchiyama, Y., Kurachi, Y., 1997. Expression and clustered distribution of an inwardly rectifying potassium channel, KAB-2/Kir4.1, on mammalian retinal Muller cell membrane: their regulation by insulin and laminin signals. *J. Neurosci.* 17, 7725–7735.
- Isomoto, S., Kondo, C., Kurachi, Y., 1997. Inwardly rectifying potassium channels: their molecular heterogeneity and function. *Jpn. J. Physiol.* 47, 11–39.
- Kharkovets, T., Hardelin, J.P., Safieddine, S., Schweizer, M., El-Amraoui, A., Petit, C., Jentsch, T.J., 2000. KCNQ4, a K⁺ channel mutated in a form of dominant deafness, is expressed in the inner ear and the central auditory pathway. *Proc. Natl. Acad. Sci. USA* 97, 4333–4338.
- Kofuji, P., Ceelen, P., Zahs, K.R., Surbeck, L.W., Lester, H.A., Newman, E.A., 2000. Genetic inactivation of an inwardly rectifying potassium channel (Kir4.1 subunit) in mice: phenotypic impact in retina. *J. Neurosci.* 20, 5733–5740.
- Kusaka, S., Horio, Y., Fujita, A., Matsushita, K., Inanobe, A., Gotow, T., Uchiyama, Y., Tano, Y., Kurachi, Y., 1999. Expression and polarized distribution of an inwardly rectifying K⁺ channel, Kir4.1, in rat retinal pigment epithelium. *J. Physiol.* 520, 373–381.
- Lagrutta, A.A., Bond, C.T., Xia, X.M., Pessia, M., Tucker, S., Adelman, J.P., 1996. Inward rectifier potassium channels. Cloning, expression and structure-function studies. *Jpn. Heart J.* 37, 651–660.
- Lee, M.P., Ravenel, J.D., Hu, R.J., Lustig, L.R., Tomaselli, G., Berger, R.D., Brandenburg, S.A., Litz, T.J., Bunton, T.E., Limb, C., Francis, H., Gorelikow, M., Gu, H., Washington, K., Argani, P., Goldenring, J.R., Coffey, R.J., Feinberg, A.P., 2000. Targeted disruption of the kvlqt1 gene causes deafness and gastric hyperplasia in mice. *J. Clin. Invest.* 106, 1447–1455.
- Marcus, D.C., Wu, T., Wangemann, P., Kofuji, P., 2002. KCNJ10 (Kir4.1) potassium channel knockout abolishes endocochlear potential. *Am. J. Physiol. Cell Physiol.* 282, C403–C407.

- Neusch, C., Rozengurt, N., Jacobs, R.E., Lester, H.A., Kofuji, P., 2001. Kir4.1 potassium channel subunit is crucial for oligodendrocyte development and in vivo myelination. *J. Neurosci.* 21, 5429–5438.
- Reimann, F., Ashcroft, F.M., 1999. Inwardly rectifying potassium channels. *Curr. Opin. Cell Biol.* 11, 503–508.
- Romey, G., Attali, B., Chouabe, C., Abitbol, I., Guillemare, E., Barhanin, J., Lazdunski, M., 1997. Molecular mechanism and functional significance of the MinK control of the KvLQT1 channel activity. *J. Biol. Chem.* 272, 16713–16716.
- Schulze-Bahr, E., Haverkamp, W., Wedekind, H., Rubie, C., Hordt, M., Borggrefe, M., Assmann, G., Breithardt, G., Funke, H., 1997. Autosomal recessive long-QT syndrome (Jervell Lange-Nielsen syndrome) is genetically heterogeneous. *Hum. Genet.* 100, 573–576.
- Takeuchi, S., Ando, M., Kakigi, A., 2000. Mechanism generating endocochlear potential: role played by intermediate cells in stria vascularis. *Biophys. J.* 79, 2572–2582.
- Takeuchi, S., Ando, M., Sato, T., Kakigi, A., 2001. Three-dimensional and ultrastructural relationships between intermediate cells and capillaries in the gerbil stria vascularis. *Hear. Res.* 155, 103–112.
- Talebizadeh, Z., Kelley, P.M., Askew, J.W., Beisel, K.W., Smith, S.D., 1999. Novel mutation in the KCNQ4 gene in a large kindred with dominant progressive hearing loss. *Hum. Mutat.* 14, 493–501.
- Van Hauwe, P., Coucke, P., Van Camp, G., 1999. The DFNA2 locus for hearing impairment: two genes regulating K⁺ ion recycling in the inner ear. *Br. J. Audiol.* 33, 285–289.
- Vetter, D.E., Mann, J.R., Wangemann, P., Liu, J., McLaughlin, K.J., Lesage, F., Marcus, D.C., Lazdunski, M., Heinemann, S.F., Barhanin, J., 1996. Inner ear defects induced by null mutation of the *isk* gene. *Neuron* 17, 1251–1264.
- Wang, Q., Bowles, N.E., Towbin, J.A., 1998. The molecular basis of long QT syndrome and prospects for therapy. *Mol. Med. Today* 4, 382–388.
- Wollnik, B., Schroeder, B.C., Kubisch, C., Esperer, H.D., Wieacker, P., Jentsch, T.J., 1997. Pathophysiological mechanisms of dominant and recessive KVLQT1 K⁺ channel mutations found in inherited cardiac arrhythmias. *Hum. Mol. Genet.* 6, 1943–1949.
- Xu, H., Cui, N., Yang, Z., Qu, Z., Jiang, C., 2000. Modulation of kir4.1 and kir5.1 by hypercapnia and intracellular acidosis. *J. Physiol.* 524 (Pt. 3), 725–735.
- Yang, Z., Xu, H., Cui, N., Qu, Z., Chanchevalap, S., Shen, W., Jiang, C., 2000. Biophysical and molecular mechanisms underlying the modulation of heteromeric Kir4.1-Kir5.1 channels by CO₂ and pH. *J. Gen. Physiol.* 116, 33–46.